PERGAMON

Automatica 38 (2002) 571–583

automatica

www.elsevier.com/locate/automatica

Halo orbit mission correction maneuvers using optimal control☆

Radu Serban[a], Wang S. Koon[b], Martin W. Lo[c], Jerrold E. Marsden[b], Linda R. Petzold[a], Shane D. Ross[b,*], Roby S. Wilson[c]

[a] *Department of Mechanical and Environmental Engineering, University of California, Santa Barbara, CA 93106, USA*
[b] *Control and Dynamical Systems, California Institute of Technology, MC 107-81, Pasadena, CA 91125, USA*
[c] *Navigation and Mission Design, Jet Propulsion Laboratory, California Institute of Technology, M/S 301-140L, 4800 Oak Grove Drive, Pasadena, CA 91109, USA*

Received 27 April 2000; received in revised form 18 January 2001; accepted 27 June 2001

Abstract

This paper addresses the computation of the required trajectory correction maneuvers for a halo orbit space mission to compensate for the launch velocity errors introduced by inaccuracies of the launch vehicle. By combining dynamical systems theory with optimal control techniques, we are able to provide a compelling portrait of the complex landscape of the trajectory design space. This approach enables automation of the analysis to perform parametric studies that simply were not available to mission designers a few years ago, such as how the magnitude of the errors and the timing of the first trajectory correction maneuver affects the correction ΔV. The impetus for combining dynamical systems theory and optimal control in this problem arises from design issues for the *Genesis Discovery Mission* being developed for NASA by the Jet Propulsion Laboratory.

Keywords: Dynamical systems; Optimal control; Halo orbit transfer; Invariant manifolds; Three-body problem; Space mission design

1. Introduction and background

1.1. The Genesis Mission

The *Genesis Discovery Mission* is a solar wind sample return mission (see Lo et al., 1998). It is one of NASA's first robotic sample return missions and is scheduled for launch in the summer of 2001 to a halo orbit in the vicinity of the Sun–Earth L_1 Lagrange point; L_1 is one of the five equilibrium points in the circular restricted three-body problem (CR3BP). Fig. 1 shows a three dimensional view of the *Genesis* trajectory.

In the standard convention, L_1 is the unstable equilibrium point between the Sun and the Earth at roughly 1.5 million km from the Earth in the direction of the Sun. Once there, the spacecraft will remain in a halo orbit for two years to collect solar wind samples before returning them to the Earth for study into the origins of the solar system. Fig. 1 shows the key parts of the trajectory: the transfer to the halo, the halo orbit itself, and the return to Earth. The figure is plotted in a rotating frame, which is often used in the study of the three-body problem. The frame is defined by fixing the x-axis along the Sun–Earth line, the z-axis in the direction normal to the ecliptic, and with the y-axis completing a right-handed coordinate system. Viewed from behind the Earth, the orbit appears as a halo around the Sun, hence its name (originally named for lunar halo orbits by Farquhar (1968)).

The *Genesis* trajectory is the first mission to be fully designed using dynamical systems theory (see Howell, Barden, & Lo, 1997). As Fig. 1 shows, the trajectory travels between neighborhoods of the L_1 and L_2 libration points with the purpose of returning the samples to Earth (L_2 is roughly 1.5 million km on the opposite side of the Earth from the Sun). In dynamical systems theory, this is closely related to the existence of a heteroclinic connection between the L_1 and L_2 regions. The deeper dynamical significance of the heteroclinic connection is explored in Koon, Lo, Marsden, and Ross (2000) for the planar problem, although similar phenomena are expected in the three dimensional problem.

☆ This paper was not presented at any IFAC meeting. This paper was recommended for publication in revised form by Associate Editor Kok Lay Teo under the direction of Editor Tamer Basar. This research was supported in part by the NSF-KDI grant number NSF ATM-9873133, and by the Jet Propulsion Laboratory, California Institute of Technology, under a contract with the National Aeronautics and Space Administration.

* Corresponding author.
E-mail address: shane@cds.caltech.edu (S.D. Ross).

0005-1098/02/$ - see front matter
PII: S0005-1098(01)00279-5

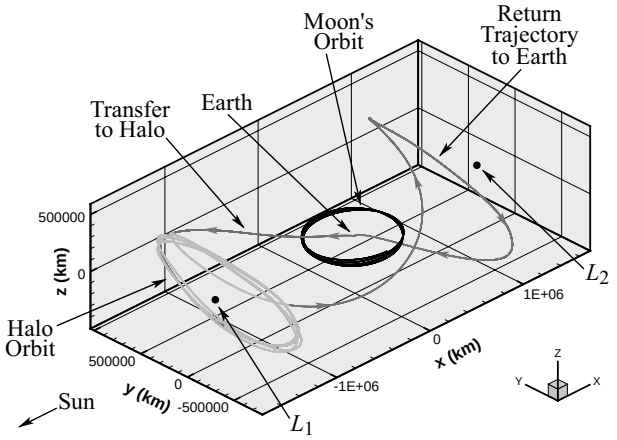

Fig. 1. The *Genesis* trajectory. The Earth is at the origin, surrounded by the Moon's orbit.

One of the attractive and interesting features of the *Genesis* trajectory design is that the three-year mission, from launch all the way back to Earth return, requires only a single small deterministic maneuver when injecting onto the halo orbit (which is actually "free", 0 m/s, in the optimal case). It is extremely difficult to use traditional classical algorithms to find such optimal and near-optimal solutions, so the design of such a low energy trajectory is facilitated by using dynamical systems methods. This is achieved by using the stable and unstable manifolds as guides in determining the end-to-end trajectory.

Our main goal in this paper is to show the feasibility of merging optimal control software with dynamical systems methods to compensate for launch vehicle errors, to which libration point missions are particularly sensitive. For this task, we have used a particular piece of software, COOPT, as our demonstration tool. There are many other good software packages which could have been used, such as MISER3, used in Liu, Teo, Jennings, and Wang (1998), and Rehbock, Teo, Jennings, and Lee (1999), and the iterative dynamic programming approach of Luus (2000). However, our goal is not to compare software packages. Rather, it is to combine dynamical systems theory with optimal control techniques to solve a sophisticated problem for an actual space mission.

1.2. Halo orbits

Halo orbits are large three-dimensional orbits shaped like the edges of a potato chip. The y-amplitude of the *Genesis* halo orbit, which extends from the x-axis to the maximum y-value of the orbit, is about 780,000 km. Note that this is bigger than the radius of the orbit of the Moon, which is about 380,000 km. The computation of halo orbits follows standard nonlinear trajectory computation algorithms based on parallel shooting. Due to the sensitivity of the problem, an accurate first guess is essential, since the halo orbit is actually an unstable orbit (albeit with a fairly long time constant in the Sun–Earth system). This first guess is provided by a high order analytic expansion of minimum third order using the Lindstedt–Poincaré method. For details of halo orbit computations and general algorithms, see Richardson (1980) and Howell and Pernicka (1988).

In the CR3BP model, which is a time independent system, halo orbits are purely periodic solutions. However, if we take into account all the perturbative effects of the full solar system model, the periodic solution ceases to exist and in its place are quasiperiodic solutions nearby in phase space. For convenience, we still refer to these solutions which shadow the periodic solutions of the simpler model as "halo" orbits.

The halo orbit is an unstable orbit, behaving dynamically like a saddle point in the directions of spectrally unstable and stable eigenvalues. There is a family of asymptotic trajectories that departs from the halo orbit called the unstable manifold and also a family of asymptotic trajectories which wind onto the halo orbit called the stable manifold. Each of these families form a two-dimensional surface that is, roughly speaking, a twisted tubular surface emanating from the halo orbit.

For *Genesis*, these manifolds are absolutely crucial to return the samples to Earth and land at the specified site, the Utah Test and Training Range. The stable manifold, which winds onto the halo orbit, is used to design the transfer trajectory which delivers the *Genesis* spacecraft from launch to halo orbit insertion (HOI). The unstable manifold, which winds off of the halo orbit, is used to design the return trajectory which brings the spacecraft and its precious samples back to Earth via the nearly heteroclinic connection. See Koon et al. (2000) for the current state of the computation of homoclinic and heteroclinic orbits in this problem.

1.3. The transfer to the halo orbit

The transfer trajectory is designed using the following procedure. A halo orbit $H(t)$ is first selected, where t represents time. The stable manifold of H, denoted W^s, consists of a family of asymptotic trajectories which take infinite time to wind onto H. However, there is a family of trajectories that lie arbitrarily close to W^s that require just a few months to transfer between Earth and the halo orbit. These trajectories are said to shadow the stable manifold. It is these shadow trajectories that we can compute and that are extremely useful to the design of the *Genesis* transfer trajectory.

A simple way to compute an approximation of W^s is based on Floquet theory. The basic idea is to linearize the equations of motion about the periodic orbit and then use the monodromy matrix provided by Floquet theory to generate a linear approximation of the stable manifold associated with the halo orbit. The linear approximation, in the form of a state vector, is integrated in the nonlinear equations of motion to produce the approximation of the stable manifold. In the case of quasiperiodic orbits that are not too far from

periodic orbits, one approximates the orbit as periodic and the same algorithm is applied to compute approximations of W^s (see Howell et al., 1997; Gómez, Masdemont, and Simó, 1993).

In this paper, we will assume that the halo orbit, $H(t)$, and the stable manifold $M(t)$ are fixed and provided. Hence we will not dwell further on the theory of their computation which is well covered in the references (see Howell et al., 1997). Instead, let us turn our attention to the trajectory correction maneuver (TCM) problem.

1.4. The trajectory correction maneuver

Genesis will be launched from a Delta 7326 launch vehicle using a Thiakol Star37 motor as the final upper stage. The most important error introduced by the inaccuracies of the launch vehicle is the velocity magnitude error. In this case, the expected error is 7 m/s (1 sigma value) relative to a boost of approximately 3200 m/s from a circular 200 km altitude Earth orbit. In the space industry, the change in velocity is called the ΔV. It is typical in space missions to use the magnitude of the required ΔV as a measure of spacecraft fuel performance.

Although a 7 m/s error for a 3200 m/s maneuver may seem small, it actually is considered quite large. Unfortunately, one of the characteristics of halo orbit missions is that, unlike interplanetary mission launches, they are extremely sensitive to launch errors. Typical interplanetary launches can correct launch vehicle errors 7–14 days after the launch. In contrast, halo orbit missions must generally correct the launch error within the first 7 days after launch or the ΔV required to correct will increase beyond the spacecraft's capability. The most important trajectory correction maneuver is called TCM1, being the first TCM of the mission. Two clean up maneuvers, TCM2 and TCM3, generally follow TCM1 after a week or more, depending on the situation. The *Genesis* ΔV budget for the TCMs is 150 m/s.

From the energy equation for a spacecraft in a conic orbit about the Earth, $E = V^2/2 - GM/R$, where E is Keplerian energy, V is velocity, GM is the gravitational mass of the Earth, and R is the distance of the spacecraft from the Earth's center, it follows that $\delta V = \delta E/V$, where δV and δE denote the variations in velocity and energy, respectively. The launch velocity error imparts an energy error δE to the spacecraft transfer orbit. In particular, for a highly elliptical orbit such as the one for *Genesis* soon after launch, V decreases sharply as a function of time since launch. Hence, the magnitude of the correction maneuver ΔV required to cancel the resulting δV grows sharply with time since launch. For a large launch vehicle error, which is possible in the case of *Genesis*, the correction maneuver TCM1 can quickly grow beyond the capability of the spacecraft's propulsion system.

The computation of TCMs is performed on the ground, relying upon accurate knowledge of the spacecraft's position and velocity. The time necessary for initial spacecraft checkout procedures, which frequently require several days after launch, compel us to investigate the effect of delays in the timing of TCM1. To thoroughly check out the spacecraft's position, velocity, and condition, it is desirable to delay TCM1 by as long as possible, even at the expense of an increased ΔV for TCM1. Consequently, the *Genesis* navigation team prefers that TCM1 be performed at 2–7 days after launch, or later if at all possible.

The design of the current *Genesis* TCM1 retargets the state after launch back to the nominal HOI state (see Lo et al., 1998). This approach is based on linear analysis and is adequate only if TCM1 were to be performed within 24 h after launch. But as emphasized, this will not be the case for *Genesis*, which can permit a TCM1 only after 24 h past launch, and probably more like 2–7 days past launch.

The requirement of a relatively long time delay between launch (when error is imparted) and TCM1 (when error is corrected) suggests that one use a nonlinear approach, combining dynamical systems theory with optimal control techniques. We explore two similar but slightly different approaches and are able to obtain in both cases an optimal maneuver strategy that fits within the *Genesis* ΔV budget of 150 m/s for the transfer portion of the trajectory. These are:

(1) HOI technique: use optimal control techniques to retarget the halo orbit with the original nominal trajectory as the initial guess.
(2) MOI technique: target the stable manifold.

Both methods are shown to yield good results.

2. Optimal control for trajectory correction maneuvers

We now introduce the general problem of optimal control for the spacecraft trajectory planning problem. We start by recasting the TCM problem as a spacecraft trajectory planning problem. Mathematically they are exactly the same. We discuss the spacecraft trajectory planning problem as an optimization problem and highlight the formulation characteristics and particular solution requirements. Then the loss in fuel efficiency caused by possible perturbation in the launch velocity and by different delays in TCM1 is exactly the sensitivity analysis of the optimal solution. COOPT, the software we use, is an excellent tool in solving this type of problem, both in providing a solution for the trajectory planning problem with optimal control, and in studying the sensitivity of different parameters.

We emphasize that the objective in this work is not to design the original nominal transfer trajectory, but rather to investigate recovery issues related to possible launch velocity errors which cause the spacecraft to deviate from the nominal trajectory. We therefore assume that a nominal transfer trajectory (corresponding to zero errors in launch velocity) is available. For the nominal trajectory in our

numerical experiments in this paper, we do not use the actual *Genesis* mission transfer trajectory, but rather an approximation obtained with a more restricted model, which has single maneuver of about 13 m/s at the point of insertion onto the halo orbit. It has been shown elsewhere (e.g., Howell et al., 1997) that the general qualitative characteristics found in the restricted models translate well when extended into more accurate models; we expect the same correlation with this work.

2.1. Recasting TCM as a trajectory planning problem

Although different from a dynamical systems perspective, the HOI and MOI problems are very similar once cast as optimization problems. In the HOI problem, a final maneuver (jump in velocity) is allowed at $T_{\mathrm{HOI}} = t_{\max}$, while in the MOI problem, the final maneuver takes place on the stable manifold at $T_{\mathrm{MOI}} < t_{\max}$ and no maneuver is allowed at $T_{\mathrm{HOI}} = t_{\max}$. A halo orbit insertion trajectory design problem can be simply posed as the following.

> Statement of the problem: *Find the maneuver times and sizes to minimize fuel consumption* (ΔV) *for a trajectory starting near Earth and ending on the specified halo orbit around the Lagrange point* L_1 *of the Sun–Earth system at a position and with a velocity consistent with the HOI time.*

One can think of the TCM problem as a rendezvous problem. After launch, and the subsequent launch error, the actual spacecraft goes off the nominal trajectory. Since placement of the spacecraft on the nominal trajectory at the appropriate location *and time* is important for our problem, imagine that a virtual spacecraft remains on the nominal trajectory (corresponding to zero launch error). Our goal then is to perform maneuvers such that the actual spacecraft will rendezvous with the virtual spacecraft on the nominal trajectory. From the rendezvous point onward, the actual spacecraft will then be on the nominal trajectory.

The optimization problem as stated has two important features. First, it involves discontinuous controls, since the impulsive maneuvers are represented by jumps in the velocity of the spacecraft. A reformulation of the problem to cast it into the framework required by continuous optimal control algorithms will be discussed later in this section. Secondly, the final halo orbit insertion time T_{HOI}, as well as all intermediate maneuver times, must be included among the optimization parameters ($\mathbf{p}$). This too requires further reformulation of the dynamical model to capture the influence of these parameters on the solution at a given optimization iteration.

Next, we discuss the reformulations required to solve the HOI discontinuous control problem; modifications of the following procedure required to solve the MOI problem are discussed in Section 3.2. We assume that the evolution of the spacecraft is described by the equations of motion

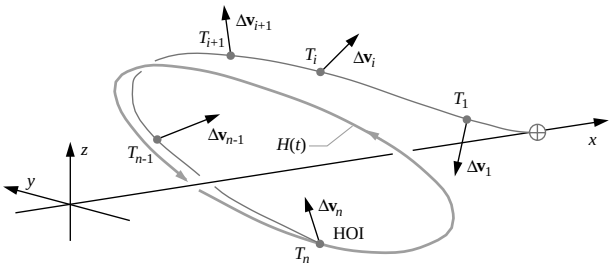

Fig. 2. Transfer trajectory. Maneuvers take place at times T_i, $i=1,2,\ldots,n$. In the stable manifold insertion problem, there is no maneuver at T_n, i.e. $\Delta\mathbf{v}_n = \mathbf{0}$.

(e.o.m.), a generic set of six ODEs $\dot{\mathbf{x}} = \mathbf{f}(t,\mathbf{x})$, where $\mathbf{x} = (\mathbf{x}^{\mathrm{p}};\mathbf{x}^{\mathrm{v}}) \in \mathbb{R}^6$ contains both positions ($\mathbf{x}^{\mathrm{p}}$) and velocities ($\mathbf{x}^{\mathrm{v}}$). The dynamical model giving the e.o.m. can be either the CR3BP or a more complex model that incorporates the influence of the Moon and other planets. In this paper, we use the CR3BP approximation; other models will be investigated in future work.

To deal with the discontinuous nature of the impulsive control maneuvers, the e.o.m. are solved simultaneously on each interval between two maneuvers. Let the maneuvers $M_1, M_2, \ldots, M_n$ take place at times T_i, $i = 1,2,\ldots,n$ and let $\mathbf{x}_i(t)$, $t \in [T_{i-1}, T_i]$ be the solution of the e.o.m. on the interval $[T_{i-1}, T_i]$ (see Fig. 2).

To capture the influence of the maneuver times on the solution of the e.o.m. and to be able to solve the e.o.m. simultaneously, we scale the time in each interval by the duration $\Delta T_i = T_i - T_{i-1}$. This is a standard technique for optimizing over the final integration time. As a consequence, all time derivatives in the e.o.m. are scaled by $1/\Delta T_i$. The dimension of the dynamical system is thus increased to $6n$.

Position continuity constraints are imposed at each maneuver and in addition, the final position is forced to lie on the given halo orbit (or stable manifold) at the proper time, that is,

$$\mathbf{x}_i^{\mathrm{p}}(T_i) = \mathbf{x}_{i+1}^{\mathrm{p}}(T_i), \quad i = 1,2,\ldots,n-1, \tag{1a}$$

$$\mathbf{x}_n^{\mathrm{p}}(T_n) = \mathbf{x}_{\mathrm{H}}^{\mathrm{p}}(T_n), \tag{1b}$$

where the halo orbit is parameterized by the HOI time T_n. Recall that the halo orbit, $H(t) = (\mathbf{x}_{\mathrm{H}}^{\mathrm{p}}(t);\mathbf{x}_{\mathrm{H}}^{\mathrm{v}}(t))$, (and also the stable manifold $M(t)$), is fixed and provided. Eq. (1b) is the constraint for the rendezvous problem at hand. If the insertion phase were not imposed, then the position on the halo orbit would be parameterized by an independent variable, i.e., the right-hand side of Eq. (1b) would be $\mathbf{x}_{\mathrm{H}}^{\mathrm{p}}(\tau)$ where τ is a free optimization parameter.

Additional constraints dictate that the first maneuver (TCM1) is delayed by at least a prescribed amount $\mathrm{TCM1}_{\min}$ and that the order of maneuvers is respected, that is,

$$T_1 \geqslant \mathrm{TCM1}_{\min}, \tag{2a}$$

$$T_{i-1} < T_i < T_{i+1}, \quad i = 1,2,\ldots,n-1. \tag{2b}$$

With a cost function defined as some measure of the velocity discontinuities

$$\begin{aligned}\Delta\mathbf{v}_i &= \mathbf{x}^{\mathrm{v}}_{i+1}(T_i) - \mathbf{x}^{\mathrm{v}}_i(T_i), \quad i = 1,2,\ldots,n-1,\\ \Delta\mathbf{v}_n &= \mathbf{x}^{\mathrm{v}}_{\mathrm{H}}(T_n) - \mathbf{x}^{\mathrm{v}}_n(T_n),\end{aligned} \tag{3}$$

the optimization problem becomes

$$\min_{T_i,\mathbf{x}_i,\Delta\mathbf{v}_i} C(\Delta\mathbf{v}_i), \tag{4}$$

subject to the constraints in Eqs. (1)–(3). Note that velocities at the intermediate maneuver points and the final insertion point are matched using bursts $\Delta\mathbf{v}_i$, $i = 1,2,\ldots,n-1$, and $\mathbf{v}_n$, respectively. More details on selecting the form of the cost function are given in Section 3.

2.2. Launch errors and sensitivity analysis

In many optimal control problems, obtaining an optimal solution is not the only goal. The influence of problem parameters on the optimal solution (the so called sensitivity of the optimal solution) is also needed. Sensitivity information provides a first-order approximation to the behavior of the optimal solution when parameters are not at their optimal values or when constraints are slightly violated.

In the problems treated in this paper, for example, we are interested in estimating the changes in fuel efficiency (ΔV) caused by possible perturbations in the launch velocity ($\varepsilon^{\mathrm{v}}_0$) and by different delays in the first maneuver (TCM1). As we show in Section 3, the cost function is very close to being linear in these parameters ($\mathrm{TCM1}_{\min}$ and $\varepsilon^{\mathrm{v}}_0$). Therefore, evaluating the sensitivity of the optimal cost is a very inexpensive and accurate method of assessing the influence of different parameters on the optimal trajectory (especially in our problem).

In COOPT, we make use of the Sensitivity Theorem (see Bertsekas, 1995) for nonlinear programming problems with equality and/or inequality constraints:

Theorem 2.1. *Let f, h, and g be twice continuously differentiable and consider the family of problems*

$$\begin{aligned}&\textit{minimize } f(x)\\ &\textit{subject to } h(x) = u, \quad g(x) \leqslant v,\end{aligned} \tag{5}$$

parameterized by the vectors $u \in \mathbb{R}^m$ and $v \in \mathbb{R}^r$. Assume that for $(u,v) = (0,0)$ this problem has a local minimum x^*, which is regular and which together with its associated Lagrange multiplier vectors λ^* and μ^*, satisfies the second order sufficiency conditions. Then there exists an open sphere S centered at $(u,v) = (0,0)$ such that for every $(u,v) \in S$ there is an $x(u,v) \in \mathbb{R}^n$, $\lambda(u,v) \in \mathbb{R}^m$, and $\mu(u,v) \in \mathbb{R}^r$, which are a local minimum and associated Lagrange multipliers of problem (5). Furthermore, $x(\cdot)$, $\lambda(\cdot)$, and $\mu(\cdot)$ are continuously differentiable in S and we have $x(0,0) = x^*, \lambda(0,0) = \lambda^*, \mu(0,0) = \mu^*$. In addition, for all $(u,v) \in S$, there holds $\nabla_u p(u,v) = -\lambda(u,v)$ and $\nabla_v p(u,v) = -\mu(u,v)$ where $p(u,v) = f(x(u,v))$ is the optimal cost parameterized by (u,v).

The influence of delaying the maneuver TCM1 is thus directly computed from the Lagrange multiplier associated with the constraint of Eq. (2a). To evaluate sensitivities of the cost function with respect to perturbations in the launch velocity ($\varepsilon^{\mathrm{v}}_0$), we must include this perturbation explicitly as an optimization parameter and fix it to some prescribed value through an equality constraint. That is, the launch velocity is set to $\mathbf{v}(0) = \mathbf{v}^{\mathrm{nom}}_0(1 + \varepsilon^{\mathrm{v}}_0/||\mathbf{v}^{\mathrm{nom}}_0||)$, where $\mathbf{v}^{\mathrm{nom}}_0$ is the nominal launch velocity and $\varepsilon^{\mathrm{v}}_0 = \varepsilon$, for a given ε. The Lagrange multiplier associated with the constraint $\varepsilon^{\mathrm{v}}_0 = \varepsilon$ yields the desired sensitivity.

2.3. Description of the COOPT software

COOPT is a software package for optimal control and optimization of systems modeled by differential-algebraic equations (DAE) (see Brenan, Campbell, & Petzold, 1995), developed by the Computational Science and Engineering Group at the University of California, Santa Barbara. It has been designed to control and optimize a general class of DAE systems. Here, we describe the basic methods used in COOPT. We consider the DAE system $\mathbf{F}(t,\mathbf{x},\dot{\mathbf{x}},\mathbf{p},\mathbf{u}(t)) = \mathbf{0}, \mathbf{x}(t_1,\mathbf{r}) = \mathbf{x}_1(\mathbf{r})$, where the DAE is index zero, one, or semi-explicit index two (see Ascher & Petzold, 1998 or Brenan et al., 1995) and the initial conditions have been chosen so that they are consistent (that is, the constraints of the DAE are satisfied). The control parameters $\mathbf{p}$ and $\mathbf{r}$ and the vector-valued control function $\mathbf{u}(t)$ must be determined such that the objective function $\int_{t_1}^{t_{\max}} \Psi(t,\mathbf{x}(t),\mathbf{p},\mathbf{u}(t))\,\mathrm{d}t + \Theta(t_{\max},\mathbf{x}(t_{\max}),\mathbf{p},\mathbf{r})$, is minimized and some additional equality and/or inequality constraints $\mathbf{g}(t,\mathbf{x}(t),\mathbf{p},\mathbf{r},\mathbf{u}(t)) \gtreqless 0$, are satisfied. The optimal control function $\mathbf{u}^*(t)$ is assumed to be continuous. To represent $\mathbf{u}(t)$ in a low-dimensional vector space, we use piecewise polynomials on $[t_1, t_{\max}]$, where their coefficients are determined by the optimization. For ease of presentation we can therefore assume that the vector $\mathbf{p}$ contains both the parameters and these coefficients and discard the control function $\mathbf{u}(t)$ in the remainder of this section. Also, we consider that the initial states are fixed and therefore discard the parameters $\mathbf{r}$ from the formulation of the optimal control problem. Hence, we consider

$$\mathbf{F}(t,\mathbf{x},\dot{\mathbf{x}},\mathbf{p}) = 0, \quad \mathbf{x}(t_1) = \mathbf{x}_1, \tag{6a}$$

$$\min \int_{t_1}^{t_{\max}} \psi(t,\mathbf{x}(t),\mathbf{p})\,\mathrm{d}t + \Theta(t_{\max},\mathbf{x}(t_{\max}),\mathbf{p}), \tag{6b}$$

$$\mathbf{g}(t,\mathbf{x}(t),\mathbf{p}) \gtreqless 0. \tag{6c}$$

There are a number of well-known methods for direct discretization of the optimal control problem in Eqs. (6),

for the case in which the DAEs can be reduced to ordinary differential equations (ODEs) in standard form. COOPT implements the single shooting method and a modified version of the multiple shooting method, both of which allow the use of adaptive DAE software.

In the multiple shooting method, the time interval $[t_1, t_{\max}]$ is divided into subintervals $[t_i, t_{i+1}]$ $(i = 1, \ldots, N_{tx})$, and the differential equations in Eq. (6a) are solved over each subinterval, where additional intermediate variables $\mathbf{X}_i$ are introduced. On each subinterval we denote the solution at time t of Eq. (6a) with initial value $\mathbf{X}_i$ at t_i by $\mathbf{x}(t, t_i, \mathbf{X}_i, \mathbf{p})$.

Continuity between subintervals in the multiple shooting method is achieved via the continuity constraints $\mathbf{C}_1^i(\mathbf{X}_{i+1}, \mathbf{X}_i, \mathbf{p}) \equiv \mathbf{X}_{i+1} - \mathbf{x}(t_{i+1}, t_i, \mathbf{X}_i, \mathbf{p}) = 0$.

The additional constraints of Eq. (6c) are required to be satisfied at the boundaries of the shooting intervals $\mathbf{C}_2^i(\mathbf{X}_i, \mathbf{p}) \equiv \mathbf{g}(t_i, \mathbf{X}_i, \mathbf{p}) \gtrless 0$. Following common practice, we write $\Phi(t) = \int_{t_1}^{t} \psi(\tau, \mathbf{x}(\tau), \mathbf{p})\, \mathrm{d}\tau$, which satisfies $\Phi'(t) = \psi(t, \mathbf{x}(t), \mathbf{p})$, $\Phi(t_1) = 0$. This introduces another equation and variable into the differential system in Eq. (6a). The discretized optimal control problem becomes

$$\begin{aligned} &\min_{\mathbf{X}_2, \ldots, \mathbf{X}_{Ntx}, \mathbf{p}} \quad \Phi(t_{\max}) + \Theta(t_{\max}), \\ &\text{s.t.} \qquad \mathbf{C}_1^i(\mathbf{X}_{i+1}, \mathbf{X}_i, \mathbf{p}) = \mathbf{0} \quad \textit{and} \quad \mathbf{C}_2^i(\mathbf{X}_i, \mathbf{p}) \gtrless 0. \end{aligned} \tag{7}$$

This problem can be solved by an optimization algorithm. We use the solver SNOPT (see Gill, Murray, & Saunders, 1997), which incorporates a sequential quadratic programming (SQP) method. The SQP methods require a gradient and Jacobian matrix that are the derivatives of the objective function and constraints with respect to the optimization variables. We compute these derivatives via DAE sensitivity software DASPK3.0 (Li & Petzold, 2000). The sensitivity equations to be solved by DASPK3.0 are generated via the automatic differentiation software ADIFOR (see Bischof, Carle, Corliss, Griewank, & Hovland, 1992).

This basic multiple-shooting type of strategy can work very well for small-to-moderate size ODE systems, and has an additional advantage that it is inherently parallel. However, for large-scale ODE and DAE systems there is a problem because the computational complexity grows rapidly with the dimension of the ODE system. COOPT implements a highly efficient modified multiple shooting method (Gill, Jay, Leonard, Petzold, & Sharma, 2000; Serban and Petzold, 2000) which reduces the computational complexity to that of single shooting for large-scale problems. However, we have found it sufficient to use single shooting for the trajectory design problems treated in this paper.

3. Numerical results

Circular restricted three-body problem: As mentioned earlier, we use the e.o.m. derived under the CR3BP assumption as the underlying dynamical model. In this model, it is assumed that the primaries (the Earth and Sun in our case) move on circular orbits around the center of mass of the system and that the third body (the spacecraft) does not influence the motion of the primaries. We write the e.o.m. in a rotating frame, as in Fig. 3.

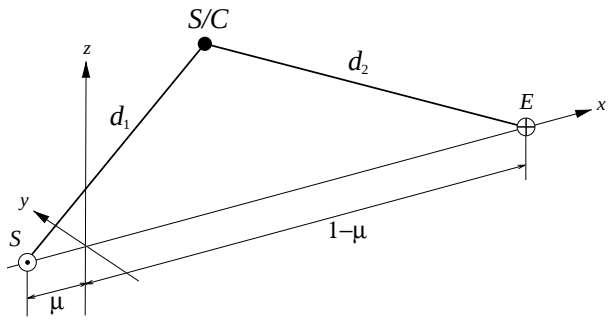

Fig. 3. Coordinate frame in the CR3BP approximation.

Using nondimensional units, the e.o.m. in the CR3BP model are

$$\begin{aligned} &\dot{x}_1 = x_4, \quad \dot{x}_4 = 2x_2 + \frac{\partial U}{\partial x_1}, \\ &\dot{x}_2 = x_5, \quad \dot{x}_5 = -2x_1 + \frac{\partial U}{\partial x_2}, \\ &\dot{x}_3 = x_6, \quad \dot{x}_6 = \frac{\partial U}{\partial x_3}, \end{aligned} \tag{8}$$

where $\mathbf{x} = [x_1, x_2, x_3, x_4, x_5, x_6]^{\mathrm{T}} = [x, y, z, v_x, v_y, v_z]^{\mathrm{T}}$, $U = \frac{1}{2}(x_1^2 + x_2^2) + (1-\mu)/d_1 + \mu/d_2$, with $d_1 = ((x_1 + \mu)^2 + x_2^2 + x_3^2)^{1/2}$ and $d_2 = ((x_1 - 1 + \mu)^2 + x_2^2 + x_3^2)^{1/2}$, and $\mu = 3.03591 \times 10^{-6}$ is the ratio between the mass of the Earth and the mass of the Sun–Earth system. In the above equations, time is scaled by the period of the primaries orbits ($T/2\pi$, where $T = 1$ year), positions are scaled by the Sun–Earth distance ($L \equiv d_{\oplus\odot} = 1.49597927 \times 10^8$ km), and velocities are scaled by the Earth's average orbital speed around the Sun ($2\pi L/T = 29.80567$ km/s).

Choice of cost function: At this point we need to give some more details on the choice of an appropriate cost function for the optimization problem (4). The spacecraft performance is measured in terms of the maneuver sizes $\Delta\mathbf{v}_i$. We consider the following two cost functions, $C_1(\Delta\mathbf{v}) = \sum_{i=1}^{n} ||\Delta\mathbf{v}_i||^2$ and $C_2(\Delta\mathbf{v}) = \sum_{i=1}^{n} ||\Delta\mathbf{v}_i||$, where $||\cdot||$ denotes the usual Euclidean norm.

The second of these is physically the most meaningful, as it measures the total sum of the maneuver sizes, but such a cost function is nondifferentiable whenever one of the maneuvers vanishes. This problem occurs already at the first optimization iteration, as the initial guess transfer trajectory only has a single nonzero maneuver at halo insertion. The first cost function, however, is differentiable everywhere.

The cost function C_1 is more appropriate for the optimizer, but it raises two new problems. It is not as physically

meaningful as the cost function C_2, and in some cases, decreasing C_1 may leads to increases in C_2.

To resolve these issues, we use the following three-stage optimization sequence:

(1) Starting with the nominal transfer trajectory as initial guess, and allowing n maneuvers, we minimize C_1 to obtain a first optimal trajectory, $\mathscr{T}_1^*$.
(2) Using $\mathscr{T}_1^*$ as initial guess, we minimize C_2 to obtain $\mathscr{T}_2^*$. During this optimization stage, some maneuvers can become very small. After each optimization iteration we monitor the feasibility of the iterate and the sizes of all maneuvers. When at least one maneuver decreases under a prescribed threshold (typically 0.1 m/s) at some feasible configuration, we stop the optimization algorithm.
(3) If necessary, a third optimization stage, using $\mathscr{T}_2^*$ as initial guess and C_2 as cost function is performed with a reduced number of maneuvers $\bar{n}$ (obtained by removing those maneuvers identified as "zero maneuvers" in step 2).

Merging optimal control with dynamical systems theory: Next, we present results for the halo orbit insertion problem (Section 3.1) and for the stable manifold insertion problem (Section 3.2). In both cases we are investigating the effect of varying times for $\mathrm{TCM1}_{\min}$ on the optimal trajectory, for given perturbations in the nominal launch velocity. The staggered optimization procedure described above is applied for values of $\mathrm{TCM1}_{\min}$ ranging from 1 to 5 day and perturbations in the magnitude of the launch velocity $\varepsilon_0^{\mathrm{v}}$ ranging from -7 m/s to $+7$ m/s. We present typical transfer trajectories, as well as the dependency of the optimal cost on the two parameters of interest. In addition, using the algorithm presented in Section 2.2, we perform a sensitivity analysis of the optimal solution. For the *Genesis* TCM problem it turns out that sensitivity information of first order is sufficient to characterize the influence of $\mathrm{TCM1}_{\min}$ and $\varepsilon_0^{\mathrm{v}}$ on the spacecraft performance.

The merging of optimal control and dynamical systems has been done through either (1) the use of the nominal transfer trajectory as a really accurate initial guess, or (2) the use of the stable invariant manifold.

3.1. Halo orbit insertion (HOI) problem

In this problem, we directly target the selected halo orbit with the last maneuver taking place at the HOI point. Using the optimization procedure described in the previous section, we compute the optimal cost transfer trajectories for various combinations of $\mathrm{TCM1}_{\min}$ and $\varepsilon_0^{\mathrm{v}}$. In all of our computations, the launch conditions are those corresponding to the nominal transfer trajectory, i.e.,

$$x_0^{\mathrm{nom}} = 1.496032475412839 \times 10^8 \text{ km}$$

$$y_0^{\mathrm{nom}} = 1.943203061350240 \times 10^3 \text{ km}$$

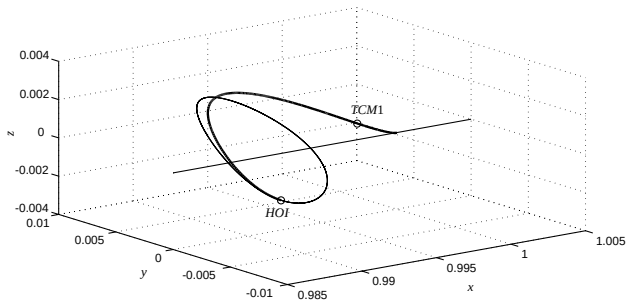

Fig. 4. HOI problem. Optimal transfer trajectory for $\mathrm{TCM1}_{\min} = 4$ days, $\varepsilon_0^{\mathrm{v}} = 3$ m/s, and $n = 4$. The optimal trajectory has $\bar{n} = 2$ maneuvers (represented by circles).

$$z_0^{\mathrm{nom}} = -2.479095822700627 \times 10^3 \text{ km}$$

$$(v_0^{\mathrm{nom}})_x = -4.612683390613825 \text{ km/s}$$

$$(v_0^{\mathrm{nom}})_y = 9.412034579485869 \text{ km/s}$$

$$(v_0^{\mathrm{nom}})_z = -3.479627336419212 \text{ km/s}$$

with the launch velocity perturbed as described in Section 2.2. These initial conditions are given in the Earth–Sun barycentered rotating frame.

As an example, we present complete results for the case in which the launch velocity is perturbed by -3 m/s and the first maneuver correction is delayed by at least 3 days. Initially, we allow for $n = 4$ maneuvers. In the first optimization stage, the second type of cost function has a value of $C_1^* = 1153.998$ (m/s)^2 after 5 iterations. This corresponds to $C_2^* = 50.9123$ m/s. During the second optimization stage, we monitor the sizes of all four maneuvers, while minimizing the cost function C_1. After 23 iterations, the optimization was interrupted at a feasible configuration when at least one maneuver decreased below a preset tolerance of 0.1 m/s. The corresponding cost function is $C_2^{**} = 45.1216$ m/s with four maneuvers of sizes 33.8252, 0.0012, 0.0003, and 11.2949 m/s. In the last optimization stage we remove the second and third maneuvers and again minimize the cost function C_2. After 7 optimization iterations an optimal solution with $C_2^{***} = 45.0292$ m/s is obtained. The two maneuvers of the optimal trajectory have sizes of 33.7002 and 11.3289 m/s and take place at 3.0000 and 110.7969 days after launch, respectively. The resulting optimal trajectory is presented in Fig. 4.

Lagrange multipliers associated with the constraints of Eq. (2a) and $\varepsilon_0^{\mathrm{v}} = \varepsilon$ give the sensitivities of the optimal solution with respect to launching velocity perturbation, -10.7341 (m/s)/(m/s), and delay in the first maneuver correction, 4.8231 (m/s)/day.

Computational and communication times: All experiments were performed on a PC workstation with an Intel Pentium III 800 MHz processor running Linux 2.2.12. The code was compiled with gcc with second level optimization. A typical run (the first optimization stage of the case

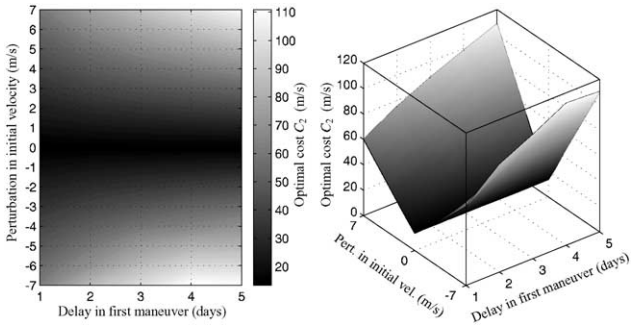

Fig. 5. HOI problem. Influence of $\mathrm{TCM1}_{\min}$ and $\varepsilon_0^{\mathrm{v}}$ on the optimal cost (C_2 in m/s) for $n = 2$.

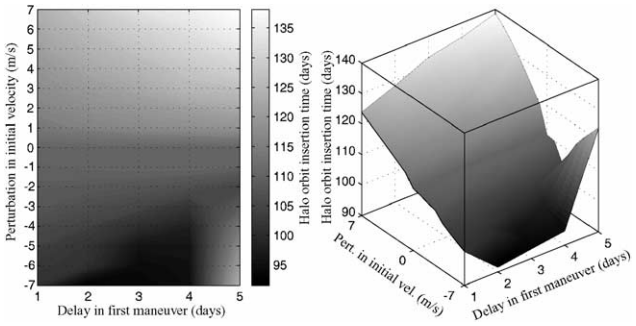

Fig. 6. HOI problem. Influence of $\mathrm{TCM1}_{\min}$ and $\varepsilon_0^{\mathrm{v}}$ on the halo orbit insertion time (T_{HOI} in days) for $n = 2$.

presented in Fig. 5) takes 0.29 s for the problem set-up and 4.23 s for the actual optimization.

For an actual TCM, this computation step is practically instantaneous. Most of the time delay is taken up before this step, by the determination of the position and velocity of the spacecraft, which reveals the launch error. Once the appropriate maneuver has been computed on the ground, it takes only a matter of seconds to communicate the maneuver information to the spacecraft.

Accuracy: We want to compute maneuvers at least as accurately as they can be implemented, given the accuracy to which the spacecraft's position and velocity can be measured. For *Genesis*, the measurement accuracy is about 1 km for position and about 0.01 m/s for velocity. For all of our computations, the integration accuracy was well within these measurement limits.

Launch errors and sensitivity analysis. The staggered optimization procedure is applied for all values of $\mathrm{TCM1}_{\min}$ and $\varepsilon_0^{\mathrm{v}}$ in the regime of interest. In a first experiment, we investigate the possibility of correcting for errors in the launch velocity using at most two maneuvers ($n = 2$). The surface of optimal cost (C_2 in m/s) as a function of these two parameters is presented in Fig. 5. Numerical values are given in Table 1.

Except for the cases in which there is no error in the launch velocity (and for which the final optimal transfer trajectories have only one maneuver at HOI), the first correction maneuver is always on the prescribed lower bound $\mathrm{TCM1}_{\min}$. The evolution of the time at which the halo insertion maneuver takes place as a function of the two parameters considered is shown in Fig. 6.

Recalling that the nominal transfer trajectory has $T_{\mathrm{HOI}} = 110.2$ days, it follows that, for all cases investigated, halo orbit insertion takes place at most 18.6 days earlier or 28.3 days later than in the nominal case.

Several important observations can be drawn from these results. First, it can be seen that, for all cases that we investigated, the optimal costs are well within the ΔV budget allocated for trajectory correction maneuvers (150 m/s for the *Genesis* mission). Secondly, as the second plot in Fig. 5 shows, the cost function surface is very close to being linear with respect to both $\mathrm{TCM1}_{\min}$ time and launch velocity

Table 1
HOI problem. Optimal costs (C_2 in m/s) for different launch velocity perturbations and delays in TCM1 for $n = 2$

$\varepsilon_0^{\mathrm{v}}$	TCM1 (days)				
(m/s)	1	2	3	4	5
−7	64.8086	76.0845	88.4296	99.6005	109.9305
−6	54.0461	67.0226	77.7832	86.8630	95.8202
−5	47.1839	57.9451	66.6277	74.4544	81.8284
−4	40.2710	48.8619	55.8274	62.0412	67.9439
−3	33.4476	39.8919	45.0290	49.6804	54.1350
−2	26.6811	30.9617	34.3489	37.3922	40.3945
−1	19.9881	22.2715	23.7848	25.2468	26.6662
0	13.4831	13.3530	13.4606	13.3465	13.2919
1	23.1900	21.9242	23.2003	24.4154	25.5136
2	26.2928	30.2773	33.3203	35.9203	38.3337
3	34.6338	38.8496	43.5486	47.7200	51.6085
4	41.4230	47.5266	53.9557	62.3780	65.1411
5	45.9268	56.2245	64.4292	75.0188	81.4325
6	53.9004	64.9741	76.6978	83.8795	95.2313
7	61.4084	75.9169	85.4875	98.4197	106.0411

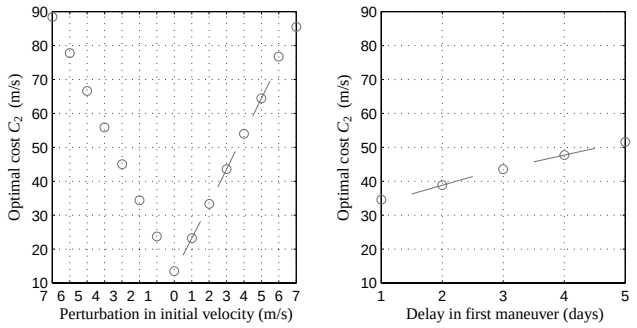

Fig. 7. HOI problem. Sensitivity of the optimal solution for $n=2$. Circles correspond to optimization results. Line segments are predictions based on sensitivity computations. The left figure was obtained with $\mathrm{TCM1}_{\min}=3$ days and shows the sensitivity of the optimal solution with respect to $\varepsilon_0^{\mathrm{v}}$. The right figure was obtained with $\varepsilon_0^{\mathrm{v}}=3$ m/s and shows the sensitivity of the optimal solution with respect to $\mathrm{TCM1}_{\min}$.

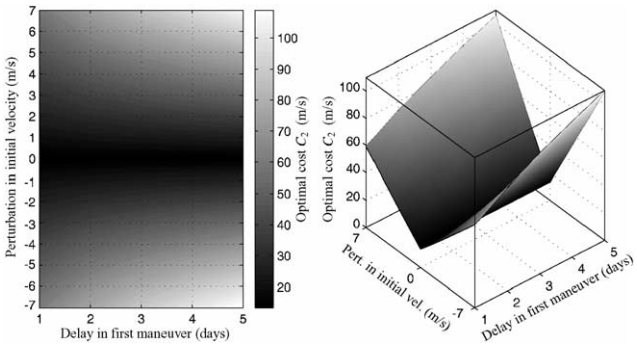

Fig. 8. HOI problem. Influence of $\mathrm{TCM1}_{\min}$ and $\varepsilon_0^{\mathrm{v}}$ on the optimal cost (C_2 in m/s). In each case, the best trajectory over $n=2,3,4$ was plotted.

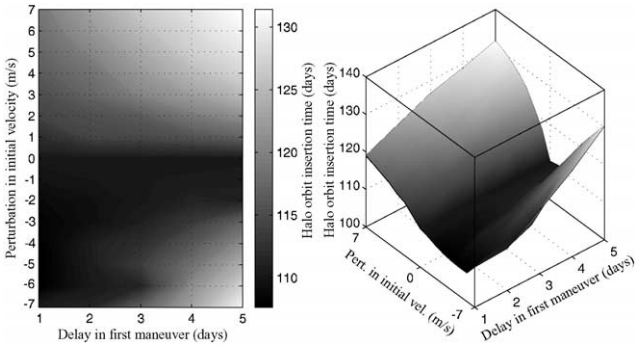

Fig. 9. HOI problem. Influence of $\mathrm{TCM1}_{\min}$ and $\varepsilon_0^{\mathrm{v}}$ on the halo orbit insertion time (T_{HOI} in days). In each case, the best trajectory over $n=2,3,4$ was plotted.

error. This suggests that first order derivative information, as obtained from sensitivity analysis of the optimal solution (Section 2.2), provides a very good approximation to the surface. For a few points on the cost function surface, we present tangents obtained from sensitivity data in Fig. 7. Finally, the halo orbit insertion time is always close enough to that of the nominal trajectory so as to not affect either the collection of the solar wind or the rest of the mission (mainly the duration for which the spacecraft evolves on the halo orbit before initiation of the return trajectory).

In a second set of numerical experiments, we allow initially for as many as $n=4$ maneuvers. This additional degree of freedom in the optimization further reduces the optimal cost function, as data in Table 2 shows.

The corresponding cost function surface is presented in Fig. 8. It is interesting to note that all optimal transfer trajectories have $\bar{n}=2$ maneuvers for negative errors in the launch velocity, $\bar{n}=1$ maneuver if there is no error, and $\bar{n}=3$ maneuvers for positive launch velocity errors. As in the previous case, the time for the first correction maneuver is always on the prescribed lower bound (i.e., $\mathrm{TCM1}=\mathrm{TCM1}_{\min}$), while the halo orbit insertion time, shown in Fig. 9, is at most 2.6 days earlier or 21.4 days later than in the nominal case.

Table 2
HOI problem. Optimal costs (C_2 in m/s) for different launch velocity perturbations and delays in first trajectory correction maneuver for the best case over $n=2,3,4$

$\varepsilon_0^{\mathrm{v}}$	TCM1 (days)				
(m/s)	1	2	3	4	5
−7	61.0946	76.0852	88.4295	99.3123	109.9174
−6	54.0461	67.0212	77.7832	86.8994	95.8202
−5	47.1389	57.9277	66.6277	74.4513	81.8572
−4	40.2710	48.8619	55.7984	62.0398	67.9438
−3	33.3664	39.8919	45.0290	49.6804	54.1357
−2	26.6720	30.9617	34.3489	37.3911	40.3945
−1	19.9674	22.1091	23.7848	25.2640	26.6618
0	13.4598	13.2902	13.4428	13.2907	13.2919
1	19.8257	21.9026	23.2005	24.4149	25.4359
2	26.2933	30.2773	33.3077	35.9203	38.3337
3	32.8151	38.8496	43.5486	47.7200	51.6085
4	39.3646	47.5279	53.9557	59.7078	65.1117
5	45.9127	56.2333	64.4292	71.7790	78.7022
6	52.4968	64.9741	74.9477	83.8795	92.3090
7	59.0967	73.7398	85.4875	95.9822	105.8960

3.2. Stable manifold orbit insertion (MOI) problem

Obtaining a good initial guess. In the MOI problem the last nonzero maneuver takes place on the stable manifold and there is no maneuver to insert onto the halo orbit. This implies that, in addition to the constraints of Eq. (1b) imposing that the final position is on the halo orbit, constraints must be imposed to match the final spacecraft velocity with the velocity on the halo orbit. These highly nonlinear constraints, together with the fact that a much larger parameter space is now investigated (we target an entire surface as opposed to just a curve) make the optimization problem much more difficult than the one corresponding to the HOI case. The first problem that arises is that the nominal transfer trajectory is not a good enough initial guess to ensure convergence to an optimum. To obtain an appropriate initial guess we use the following procedure:

(1) We start by selecting an HOI time, T_{HOI}. This yields the position and velocity on the halo orbit.
(2) The above position and velocity are perturbed in the direction of the stable manifold and the e.o.m. in Eq. (8) are integrated backwards in time for a selected duration T_{S}. This yields an MOI point which is now fixed in time, position, and velocity.
(3) For a given value of $\mathrm{TCM1}_{\min}$ and with $\varepsilon_0^{\mathrm{v}}=0$, and using the nominal transfer trajectory as initial guess, we use COOPT to find a trajectory that targets this MOI point, while minimizing C_1.

With the resulting trajectory as an initial guess and the desired value of $\varepsilon_0^{\mathrm{v}}$ we proceed with the staggered optimization presented before to obtain the final optimal trajectory for insertion on the stable manifold. During the three stages of the optimization procedure, both the MOI point and the HOI point are free to move (in position, velocity, and time) on the stable manifold surface and on the halo orbit, respectively.

The fact that we are using local optimization techniques implies that the computed optimal trajectories are very sensitive to the choice of the initial guess trajectory. For given values of the problem parameters (such as initial number of maneuvers, perturbation in launch velocity, and lower bound on TCM1) we find optimal trajectories in a neighborhood of the initial guess trajectory. In other words, computed optimal trajectories can be 'steered' towards regions of interest by appropriate choices of initial guess trajectories. For example, taking the launch time to be $T_{\mathrm{L}}=0$ and the HOI time (T^*_{HOI}) of the nominal transfer trajectory as a reference point on the halo orbit, we can investigate a given zone of the design space by an appropriate choice of the HOI point of our initial guess trajectory with respect to T^*_{HOI} (step 1 of the above procedure). That is, we select a value T_0 such that $T_{\mathrm{HOI}}=T^*_{\mathrm{HOI}}+T_0$. The point where the initial guess trajectory inserts onto the stable manifold is then defined by selecting the duration T_{S} for which the equations of motion are integrated backwards in time (step 2 of the above procedure). This gives a stable manifold insertion time of $T_{\mathrm{MOI}}=T_{\mathrm{HOI}}-T_{\mathrm{S}}=T^*_{\mathrm{HOI}}+T_0-T_{\mathrm{S}}$. Next, we use COOPT to evaluate these various choices for the initial guess trajectories (step 3 of the above procedure). A schematic of this procedure is shown in Fig. 10.

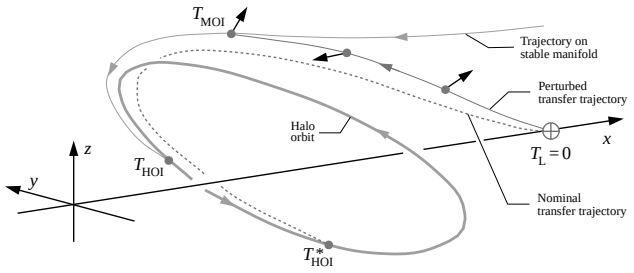

Fig. 10. MOI Problem. Description of the initial guess computation procedure.

Table 3
MOI problem. Initial guess trajectories obtained for different choices of T_0 and T_{S}. Times are in nondimensional units

T_0	T_{HOI}	T_{S}	T_{MOI}	C_2^* (m/s)
−0.25	1.65916	0.25	1.40916	45.7317
		0.50	1.15916	93.2419
		0.75	—	—
0.00	1.90916	0.25	1.65916	21.7515
		0.50	1.40916	45.1291
		0.75	1.15916	94.0839
		1.00	—	—
0.75	2.65916	0.25	2.40916	21.1051
		0.50	2.15916	21.4791
		0.75	1.90916	24.8072
		1.00	1.65916	23.9035
		1.25	1.40916	43.2514
		1.50	1.15916	86.1323
		1.75	—	—
1.50	3.40916	0.25	3.15916	15.9145
		0.50	2.90916	16.2152
		0.75	2.65916	15.6983
		1.00	2.40916	17.6370
		1.25	2.15916	27.5903
		1.50	1.90916	18.9711
		1.75	1.65916	19.4283
		2.00	1.40916	28.3686
		2.25	1.15916	51.8521
		2.50	0.90916	105.7831
		2.75	0.65916	212.9997
		3.00	0.40916	519.7044
		3.25	—	—

For different combinations of T_0 and T_{S}, Table 3 presents values of $C_2^*(\Delta\mathbf{v})=\sum_{i=1}^{n}||\Delta\mathbf{v}_i||$ corresponding to the optimal initial guess trajectory that targets the resulting MOI point. Note that, for a given value T_0, there exists a value

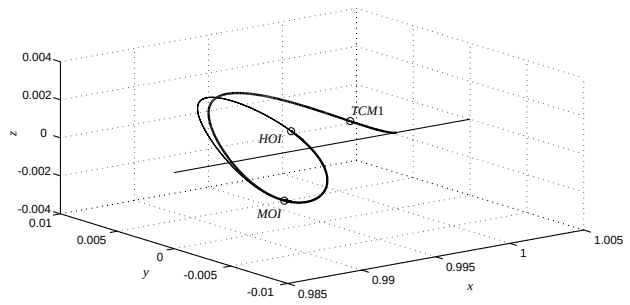

Fig. 11. MOI Problem. Optimal transfer trajectory for $\mathrm{TCM1}_{\min} = 4$ days, $\varepsilon_0^{\mathrm{v}} = -3$ m/s, and $n = 4$. The optimal trajectory has a cost function of $C_2 = 49.1817$ m/s and $\bar{n} = 2$ maneuvers. The first maneuver takes place at TCM1 = 4 days, the second one at $T_{\mathrm{MOI}} = 112.11$ days, while HOI takes place $T_{\mathrm{HOI}} = 173.25$ days after launch.

T_{S} for which we are unable to compute an initial guess trajectory. This occurs since for these values of T_0 and T_{S}, the resulting T_{MOI} is too small for COOPT to find a trajectory that targets the MOI point from $T_{\mathrm{L}} = 0$.

Regions best suited for MOI insertion: From the data given in Table 3 we can identify regions of the stable manifold that are best suited for MOI insertion. Examples of such regions are:

- (*Region A*) MOI trajectories that insert to the halo orbit in the same region as the nominal transfer trajectory and which therefore correspond to initial guess trajectories with small T_0;
- (*Region B*) MOI trajectories that have HOI points on the "far side" of the halo orbit and which correspond to initial guess trajectories with halo insertion time around $T^*_{\mathrm{HOI}} + 1.50$ ($T_0 = 174.27$ days).

These choices are confirmed by the examples from Wilson, Howell, and Lo (1999). Trajectories in the second region might, at first glance, appear unsuited for the *Genesis* mission as they would decrease the time the spacecraft is on the halo orbit (recall that design of the return trajectory dictates the time at which the spacecraft must leave the halo orbit). However, as the typical MOI trajectory of Fig. 11 shows, all trajectories on the stable manifold asymptotically wind onto the halo orbit and are thus very close to the halo orbit for a significant time. This means that collection of solar wind samples can start much earlier than halo orbit insertion, therefore providing enough time for all scientific experiments before the spacecraft leaves the halo orbit.

Once we select a region of the stable manifold by selecting an appropriate initial guess trajectory, we can perform the same type of analysis as done for the HOI problem of Section 3.1. In what follows, we consider the case in which we correct for perturbations in launch velocity by seeking optimal MOI trajectories in Region B, that is, on the far side of the halo from the Earth. For given values of $\varepsilon_0^{\mathrm{v}}$ and $\mathrm{TCM1}_{\min}$, we first compute an MOI initial guess trajectory with $T_0 = 1.50$ and $T_{\mathrm{S}} = 0.75$ and then use the staggered optimization procedure described in Section 3 to find an optimal MOI trajectory in this vicinity.

Table 4
MOI problem. Optimal costs (C_2 in m/s) for different launching velocity perturbations and delays in TCM1

$\mathrm{TCM1}_{\min}$ (days)	$\varepsilon_0^{\mathrm{v}}$ (m/s)	C_2 (m/s)
3	−3	45.1427
	−4	55.6387
	−5	65.9416
	−6	76.7144
	−7	87.3777
4	−3	49.1817
	−4	61.5221
	−5	73.4862
	−6	85.7667
	−7	99.3405
5	−3	53.9072
	−4	66.8668
	−5	81.1679
	−6	94.3630
	−7	109.2151

We present results from such computations in Table 4. The optimal MOI trajectories are very close (in terms of their associated cost function C_2) to the corresponding HOI trajectories. This can be understood by recalling that the nominal transfer trajectory that we use in our experiments actually inserts onto the halo orbit directly as opposed to the manifold. To take full advantage of the stable manifold in correcting for launching errors, one may need to start with a nominal transfer trajectory that inserts onto the stable manifold. For missions that are designed to have such nominal transfer trajectories, correction trajectories that also insert onto the stable manifold are expected to be much more efficient than those obtained with the current problem formulation.

4. Conclusions and future work

This paper explores new approaches for automated parametric studies of optimal trajectory correction maneuvers for a halo orbit mission. Using the halo orbit insertion approach, we found optimal recovery trajectories for all the launch velocity errors and $\mathrm{TCM1}_{\min}$ considered. The cost functions (fuel consumption in terms of ΔV) are within the allocated budget even in the worst case (largest launch velocity error and $\mathrm{TCM1}_{\min}$).

Using the stable manifold insertion approach, we obtained similar results to those found using HOI targeted trajectories. The failure of the MOI approach to reduce the ΔV significantly may be because the optimization procedure (even in the HOI targeted case) naturally finds trajectories 'near'

the stable manifold. We will investigate this interesting effect in future work.

The main contribution of dynamical systems theory to the problem of finding optimal recovery trajectories is in the construction of good initial guess trajectories in sensitive regions which allows the optimizer to home in on the solution. This aspect of our work will be important in many other future mission design problems. Many missions in the future will require the use of optimal control in the context of low thrust. The software and methods of this paper can be used with little change for such problems. In fact, the techniques of this paper are applicable to a variety of problems. We plan to investigate these and related issues in future publications.

Acknowledgements

This work was carried out at the Computational Science and Engineering Group at the University of California, Santa Barbara, the Jet Propulsion Laboratory and the California Institute of Technology. The work was partially supported by the Caltech President's fund, the NASA Advanced Concepts Research Program, The *Genesis* Project, NSF grant KDI/ATM-9873133 and AFOSR Microsat contract F49620-99-1-0190.

References

Ascher, U. M., & Petzold, L. R. (1998). *Computer methods for ordinary differential equations and differential-algebraic equations*. Philadelphia, PA: SIAM.

Bertsekas, D. R. (1995). *Nonlinear programming*. Belmont, MA: Athena Scientific.

Bischof, C., Carle, A., Corliss, G., Griewank, A., & Hovland, P. (1992). ADIFOR—generating derivative codes from Fortran programs. *Science Programming*, *1*(1), 11–29.

Brenan, K. E., Campbell, S. L., & Petzold, L. R. (1995). *Numerical solution of initial-value problems in differential-algebraic equation* (2nd ed.). Philadelphia, PA: SIAM.

Farquhar, R. W. (1968). *The control and use of libration-point satellites*. Ph.D. Thesis, Dept. of Aeronautics and Astronautics, Stanford University, Stanford, California, USA.

Gill, P. E., Jay, L. O., Leonard, M. W., Petzold, L. R., & Sharma, V. (2000). An SQP method for the optimal control of large-scale dynamical systems. *Journal of Computational and Applied Mathematics*, *120*(1–2), 197–213.

Gill, P. E., Murray, W., & Saunders, M. A. (1997). SNOPT: *An SQP algorithm for large-scale constrained optimization*. Numerical Analysis Report 97-2, Department of Mathematics, University of California, San Diego, La Jolla, CA.

Gómez, G., Masdemont, J., & Simó, C. (1993). Study of the transfer from the Earth to a halo orbit around the equilibrium point L_1. *Celestial Mechanics and Dynamical Astronomy*, *56*, 541–562.

Howell, K. C., Barden, B., & Lo, M. (1997). Application of dynamical systems theory to trajectory design for a libration point mission. *Journal of Astronautics Science*, *45*(2), 161–178.

Howell, K. C., & Pernicka, H. J. (1988). Numerical determination of Lissajous trajectories in the restricted three-body problem. *Celestial Mechanics*, *41*, 107–124.

Koon, W. S., Lo, M. W., Marsden, J. E., & Ross, S. D. (2000). Heteroclinic connections between periodic orbits and resonance transitions in celestial mechanics. *Chaos*, *10*(2), 427–469.

Li, S., & Petzold, L. R. (2000). Software and algorithms for sensitivity analysis of large-scale differential-algebraic systems. *Journal of Computational and Applied Mathematics*, *125*(1–2), 131–145.

Liu, Y., Teo, K. L., Jennings, L. S., & Wang, S. (1998). On a class of optimal control problems with state jumps. *Journal of Optimal Theory and Applications*, *98*(1), 65–82.

Lo, M., Williams, B. G., Bollman, W. E., Han, D., Hahn, Y., Bell, J. L., Hirst, E. A., Corwin, R. A., Hong, P. A., Howell, K. C., Barden, B., & Wilson, R. (1998). *Genesis mission design*. Paper No. AIAA 98-4468.

Luus, R. (2000). *Iterative dynamic programming*. London: CRC Press.

Rehbock, V., Teo, K. L., Jennings, L. S., & Lee, H. W. J. (1999). A survey of the control parametrization and control parametrization enhancing methods for constrained optimal control. In A. Eberhard, R. Hill, D. Ralph, & & B.M. Glover (Eds.), *Progress in Optimization; Contributions from Australia*. Dordrecht: Kluwer Academic.

Richardson, D. L. (1980). Analytic construction of periodic orbits about the collinear points. *Celestial Mechanics*, *22*, 241–253.

Serban, R., & Petzold, L. R. (2000). COOPT—A software package for optimal control of large-scale differential-algebraic equation systems. *Mathematics and Computers in Simulation*, *56*(2), 187–203.

Wilson, R. S., Howell, K. C., & Lo, M. W. (1999). *Optimization of insertion cost for transfer trajectories to libration point orbits*. Paper No. AAS 99-401.

Radu Serban was born in Sibiu, Romania in 1968. He received his M.Sc. in Aerospace Engineering from the Polytechnic Institute in Bucharest, Romania in 1992. In 1998 he received his Ph.D. in Mechanical Engineering from the University of Iowa. From 1998 to 2001 he worked as a postgraduate researcher in the Computational Science and Engineering group at the University of California Santa Barbara. In July 2001 he joined the Center for Applied Scientific Computing at Lawrence Livermore National Laboratory. His research topics include optimal control and optimization, sensitivity analysis, and multibody dynamics.

Wang Sang Koon is a Senior Postdoctoral Scholar of Control and Dynamical Systems at the California Institute of Technology. He received his Ph.D. in 1997 at the University of California, Berkeley and was awarded the Bernard Friedman Memorial Prize for the best Ph.D. Thesis in Applied Mathematics. He has done research in the area of geometric mechanics such as optimal Control for holonomic and nonholonomic mechanical systems with symmetry. His current research interests are in applied dynamics and control theory, especially in the study of formation flight for micro-satellites, and the design of optimized space missions which employ solutions of the three or more body problem.

Dr. Martin W. Lo is a member of the technical staff in the Navigation and Mission Design Section of the Jet Propulsion Laboratory, California Institute of Technology. Lo received his Ph.D. from Cornell University and his B.S. from the California Institute of Technology in mathematics. As Mission Design Manager, he led the development of the trajectory for the Genesis Mission which recently launched and is on its way to L1. He is currently leading

the development of LTool, JPL's newest mission design tool which uses dynamical systems techniques to design highly nonlinear trajectories. The Genesis Mission is the first user of LTool. He is the organizer of the Lagrange Group, an international group of researchers and engineers from universities, NASA centers, and industry whose focus is on the development of nonlinear astrodynamics techniques with applications to space missions. His interests includes mission design, the three body problem, dynamical systems theory, satellite constellation coverage analysis, dynamical astronomy, and computational mathematics.

Jerrold E. Marsden is a Professor of Control and Dynamical Systems at the California Institute of Technology. He received his B.Sc. at Toronto in 1965 and his Ph.D. at Princeton University in 1968, both in Applied Mathematics. He has done research in the area of geometric mechanics, with applications to rigid body systems, fluid mechanics, elasticity theory, plasma physics and general field theory. He is one of the founders of reduction theory for mechanical systems with symmetry. His current research interests are in applied dynamics and control theory, especially how these subjects relate to mechanical systems and systems with symmetry.

Dr. Linda R. Petzold is currently Professor in the Departments of Mechanical and Environmental Engineering, and Computer Science, and Director of the Computational Science and Engineering Program, at the University of California Santa Barbara. She was awarded the Wilkinson Prize for Numerical Software in 1991, and the Dahlquist Prize, for numerical solution of differential equations, in 1999. She is currently Vice President at Large of SIAM, the Society for Industrial and Applied Mathematics. Her research interests include numerical ordinary differential equations, differential-algebraic equations, and partial differential equations, dynamic optimization, nonlinear model reduction, mathematical software and scientific computing.

Shane D. Ross earned a B.S. in physics from the California Institute of Technology in 1998. He is currently pursuing a Ph.D. in Control and Dynamical Systems from the same university. His research interests include material transport in the solar system and the application of dynamical systems and optimal control methods to the design of fuel optimized space missions which employ solutions of the three or more body problem.

Dr. Roby S. Wilson is a member of the technical staff in the Navigation and Mission Design section of the Jet Propulsion Laboratory, California Institute of Technology. He received his B.S. in 1991, MS in 1993, and Ph.D. in 1998, all in Aeronautical and Astronautical Engineering from Purdue University. He has been involved in the development of the Genesis trajectory since 1997, and has worked extensively on the design and re-design of the mission. His interests involve trajectory design in the three and four body problems, especially those involving multiple lunar encounters. He is currently the trajectory analyst for the Genesis spacecraft operations at JPL.